Published in the Proceedings of the 16th International Aluminum Alloys Conference (ICAA16) 2018
ISBN: 978-1-926872-41-4
by the Canadian Institute of Mining, Metallurgy & Petroleum

BRAZING CHARACTERISTICS OF WARM FORMED AUTOMOTIVE HEAT EXCHANGER COMPONENTS

*M. J. Benoit[1], K. B. Han[1], M. J. Worswick[1], M. A Wells[1], and S. Winkler[2]

[1]Department of Mechanical and Mechatronics Engineering, University of Waterloo
Waterloo, Ontario, Canada
*(*Corresponding author: mjlbenoi@uwaterloo.ca)*

[2]Dana Canada Corporation,
Oakville, Ontario, Canada

ABSTRACT

Automotive heat exchangers are fabricated by forming multi-layered aluminum (Al) alloy brazing sheets into the desired geometry and subsequently passing the assembly through a furnace for brazing. As manufacturers seek to use thinner gauge and higher strength sheet to reduce vehicle weight, forming of the Al alloy sheets has become a challenge. Warm forming has previously proven to allay these forming concerns, but no consideration was given to the effect of increasing the forming temperature on brazing. Recently, it was shown that annealed sheet was more susceptible to the detrimental phenomenon of liquid film migration (LFM) during brazing if formed above 150°C, while work hardened sheets showed no increased susceptibility to LFM with increasing forming temperature, up to 250°C. In the current study, the brazing performance of simulated battery cooling plates was investigated. The plates were fabricated both from fully annealed and work hardened sheets. Brazing was assessed by microstructural evolution during a brazing cycle. The post-brazed microstructure varied with strain and forming temperature in plates made from annealed sheets, while no variation in microstructure with location or forming temperature was observed in plates formed from work hardened sheets.

KEYWORDS

Automotive, Heat exchangers, Brazing, Warm forming, Recrystallization, Strain induced boundary migration (SIBM), Liquid film migration (LFM)

INTRODUCTION

Since the 1970's, one common method of fabricating automotive heat exchangers has been by forming multi-layered aluminum (Al) alloy sheets, and subsequently brazing the formed components together in a controlled atmosphere furnace. The Al alloy sheets used are comprised of at least two Al alloys roll bonded together, but can consist of additional layers, depending on the application; at minimum, the sheets are comprised of a core and clad layer. The core layer, often an AA3xxx alloy, remains solid throughout processing and provides strength to the assembly. The clad layer is always one of the AA4xxx series alloys which, due to their high silicon (Si) content, have a melting temperature range well below that of the core alloy. When the sheet is passed through the brazing furnace, the clad alloy melts to provide the brazed joint filler metal throughout the assembly, while the core alloy remains solid.

In order to achieve cost and weight savings, heat exchanger fabricators have used Al alloy sheets with reduced thickness. However, deformation and brazing of these increasingly thin components remains a concern (Zhao & Woods, 2013). Furthermore, springback has been observed after forming sheets of higher initial strength (i.e. work hardened conditions), leading to flatness issues of formed components. Consequently, the ability to form high quality brazed joints is difficult in components formed from higher strength brazing sheets.

Warm forming, where the sheet is heated to below its recrystallization temperature before and/or during forming, has recently been shown to alleviate both of the aforementioned forming issues. Increases in the limiting strain and maximum draw depth of multi-layered Al brazing sheet were observed when the sheet was formed at 200°C and above (Bagheriasl, Ghavam, & Worswick, 2014; Bagheriasl & Worswick, 2015), while reductions in sheet springback have been found for forming at 150°C and above, particularly for work hardened sheets (Verma, George, Kurukuri, Worswick, & Winkler, 2015). Until recently however, there had been no consideration for how forming temperature could impact the post-braze microstructure. This was a critical gap in materials processing knowledge, since it is known that the pre-braze microstructure will determine the interactions between the liquid clad and solid core during brazing. Of particular interest to formed Al brazing sheet is the detrimental phenomenon of liquid film migration (LFM), where the liquid clad alloy penetrates the core along grain boundaries, reducing the remaining core alloy thickness and depleting the amount of liquid clad filler metal available for brazing (Woods, 1997). Further, the extent of LFM attack on the core has a non-linear relationship with applied strain prior to brazing, with the most severe instances of LFM occurring at low to intermediate levels of strain (Yang & Woods, 1997; Wittebrood, 2009).

Recently, the brazing performance of annealed Al brazing sheet was predicted to be impaired relative to room temperature formed sheet if formed above 150°C, due to an extension of the range of strains over which LFM could occur (Benoit, Kaur, Wells, Jin, Shalchi Amirkhiz, & Winkler, 2018). On the other hand, the brazing performance of work hardened H24 sheet, which was predicted using differential scanning calorimetry measurements during thermal cycling, was found to be insensitive to an increase in forming temperature, up to 250°C (Benoit, Whitney, Wells, Jin, & Winkler, 2017). However, these prior studies were performed using simple uniaxial tensile specimens, strained in a furnace; a more comprehensive understanding of brazing performance in components with complex geometry and multi-axial stresses is needed. Thus, the objective of the current study was to investigate the brazing performance of warm formed heat exchanger components. Specifically, simulated electric vehicle battery cooling plates were used, and brazing performance was assessed on the basis of metallurgical reactions which occur within the sheet during a simulated brazing cycle.

METHODS

Materials

Al brazing sheets were supplied in both the fully annealed (O) and work hardened and partially annealed (H24) tempers. The sheets had a nominal overall thickness of 200 µm, with a single clad alloy layer consisting of approximately 10% of the total sheet thickness. A cross section of the as-received O

temper brazing sheet is shown in Figure 1. The composition of both core and clad alloys is given in Table 1. The core alloy composition was measured using inductively coupled plasma optical emission spectrometry (ICP-OES) after the clad alloy was removed by chemical etching with sodium hydroxide (NaOH) solution. The clad composition was calculated by performing ICP-OES on the full brazing sheet, and subtracting the previously determined core composition, accounting for the weight fraction of the core layer.

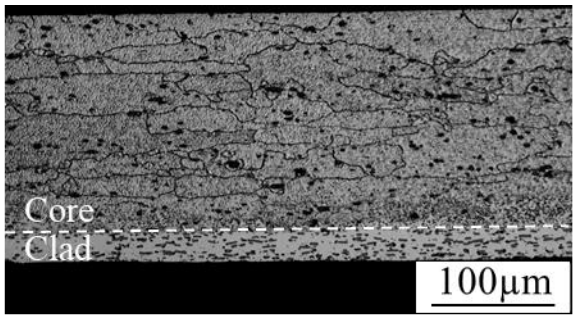

Figure 1. Al brazing sheet cross section (O temper)

Table 1. Composition in wt% of the Al alloys used in the brazing sheet (bal. Al)

Sheet Layer	Si	Mn	Cu	Fe	Other
Clad	9.19	-	0.11	0.10	≤0.08
Core	0.18	0.86	0.64	0.33	≤0.08

Sample Preparation

Brazing performance was assessed using a simulated electric vehicle battery cooling plate (Figure 2). In production, two identically formed plates would be placed with the clad alloy layers clamped together to form coolant channels and passed through a furnace to form a leak free battery cooling plate. One-half of the full battery cooling plate assembly was used to assess microstructural evolution during a brazing cycle in the current study.

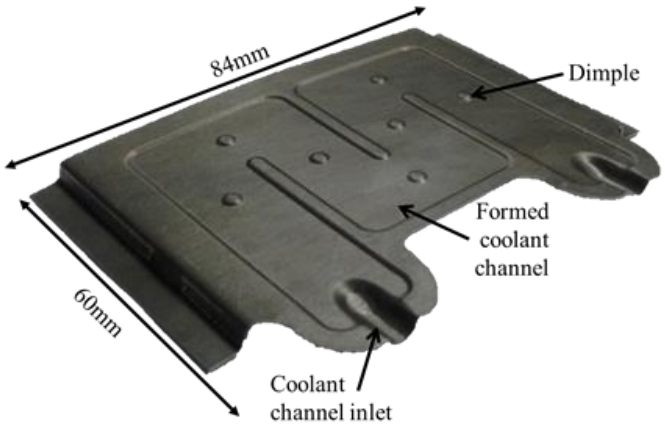

Figure 2. One half of a simulated electric vehicle battery cooling plate, with major formed features and dimensions indicated. The upper surface in this image is the clad alloy layer

Battery plates were formed from both O and H24 sheet tempers. Based on prior investigations with uniaxial specimens, O temper sheets were formed at room temperature (RT), 150°C, and 250°C, while H24 sheet was formed only at RT and 250°C. To form the plates, a custom tooling assembly mounted on

an Instron 1331 mechanical testing apparatus was used, where the punch and die were heated to and maintained at the forming temperature using cartridge heaters and thermocouples to relay temperature data to the heater controller. The core side of the brazing sheet blanks were sprayed with MS-153BN boron nitride lubricant to avoid cracking of the components during forming. Prior to forming, the punch and die were brought together such that the punch contacted the blank for 45 s to conductively heat the sheet to the desired forming temperature (Han, George, Kurukuri, Worswick, & Winkler, 2017). For RT forming, no heating step was used. After heating, forming was performed using a punch speed of 1 mm/s, punch force of 80 kN, and a hold time in the fully closed position of 2 s.

After forming, the plates were subjected to a simulated brazing cycle using a nitrogen gas controlled atmosphere furnace, where the plates were heated to a peak temperature between 590°C and 600°C, held for 3 min and then cooled. Brazing was carried out using Dana Corporation's proprietary fluxless brazing process, whereby a nickel-based braze promotor (instead of NOCOLOK® or KAlF flux) was used for oxide disruption and molten clad flow (Cheadle & Dockus, 1988).

The battery plates were sectioned at critical locations after brazing, determined using uniaxial test data from prior studies and a finite element model of the formed battery plate. The cross-sections were mounted and prepared for metallographic analysis by grinding and polishing with progressively finer sandpaper and diamond particle size, respectively. The core alloy grain structure was revealed by etching with Keller's reagent.

Battery Plate Finite Element Model

A finite element (FE) model of the battery plate was developed to predict strain throughout the plate, in order to correlate past uniaxial test data with the microstructures in the formed plate after simulated brazing. Forming simulations were performed using the LS-DYNA software (Livermore Software Technology Corporation, 2015) with a non-linear dynamic explicit formulation, in which the plate was modeled using quadrilateral shell elements 0.15 mm in size (Han, 2017). The material model used the von Mises yield surface criterion and the extended Nadai phenomenological model to capture thermal softening and strain rate sensitivity during forming at elevated temperatures. The simulations used a punch speed of 1 mm/s to match experimental conditions.

RESULTS AND DISCUSSION

Microstructural analysis was performed at two critical cross-sections in the battery plate. The first section was taken through the inlet to the coolant channel, at a distance of 4 mm from the front of the battery plate, and the second was taken through the four collinear formed dimples across the width of the battery plate. These sections are brazed joint faying surfaces in the full assembly but, unlike the flange areas surrounding the formed channels, these two sections experience a wide range of strains, which could lead to variable post-braze microstructures. Magnified images of the FE model at each of the two locations are given in Figure 3a and b. For the channel inlet cross section, microstructure analysis was performed at (1) the radius leading into the inlet where the strain is high, and (2) along the side of the inlet where the strain is comparatively lower. The microstructure at the top of the formed dimple was also investigated, where the strain was around 4% for all forming conditions which, from prior uniaxial tests, was the forming condition with the worst predicted brazing performance for the fully annealed sheet (Benoit et al., 2017). The FE membrane strain predictions along both cross-sections are given in Figure 3c and d for O temper sheet and all forming temperatures. Due to symmetry assumptions, the strain predictions in Figure 3d are shown only up to the mid-plane of the plate. The trend in strain predictions are similar for H24 sheet, although the exact values differ slightly, due to differences in the material hardening behaviour and earlier onset diffuse necking in the H24 sheet during forming at high temperature.

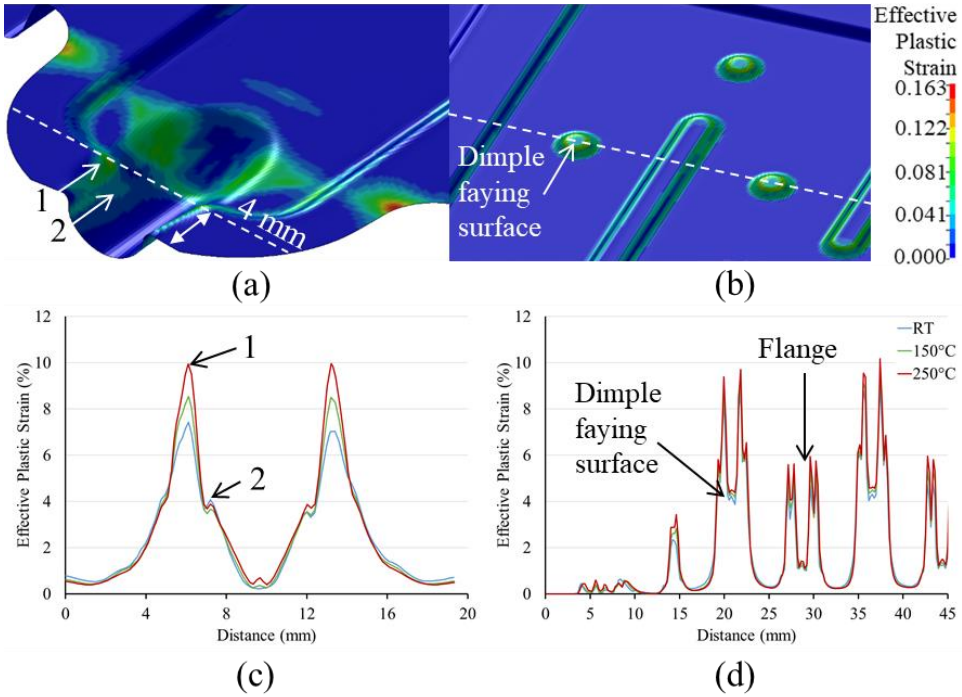

Figure 3. Magnified view of FE model (a, b) and corresponding membrane strain predictions (c, d) with locations of interest indicated at the (a, c) channel inlet and (b, d) dimple cross-sections

The post-braze microstructures at location 1 of the channel inlet (Figure 4), where the strain was estimated to be between 7.4% (RT) and 9.9% (250°C) for O temper sheet and between 10.0% (RT) and 12.9% (250°C) for H24 sheet, depended on both the forming temperature and initial sheet temper. For the RT formed O temper sheet (Figure 4a), the core alloy was characterized by coarse grains, with the grain size approaching the full sheet thickness. This coarsened microstructure has previously been attributed to strain induced boundary migration (SIBM) (Wittebrood, Desikan, Boom, & Katgerman, 2006), the dominant recrystallization mechanism in Al alloys deformed up to 20% (Bellier & Doherty, 1977). Furthermore, a thin, relatively uniform clad residue layer is present at the surface of the sheet, with no LFM observed. When the forming temperature was increased to 150°C (Figure 4b), a coarse core alloy characteristic of SIBM and uniform clad residue layer were observed at the radii of the inlet; however, directly adjacent to this region in the inlet where strain rapidly decreases (Figure 3c), a stark contrast in the microstructure was observed. The core alloy there was characterized by small, elongated grains similar to the pre-braze condition, suggesting recrystallization did not occur at this location during brazing. Furthermore, the thin residual clad layer transitioned to large, blocky grains protruding into the core layer, which are consistent with the morphology of the LFM phenomenon. A non-recrystallized core alloy and large surface grains consistent with LFM were prevalent across location 1 of the channel inlet for the plate formed at 250°C (Figure 4c). On the other hand, the core alloy of the H24 sheets, which was originally comprised of pancaked grains from prior sheet processing, recrystallized during brazing, regardless of forming temperature (Figure 4d and e). It should be noted that the recrystallized grains in the H24 sheets are finer than those characteristic of SIBM. As a consequence of core recrystallization, a uniform clad residue layer was present at the sheet surface, and no LFM was observed.

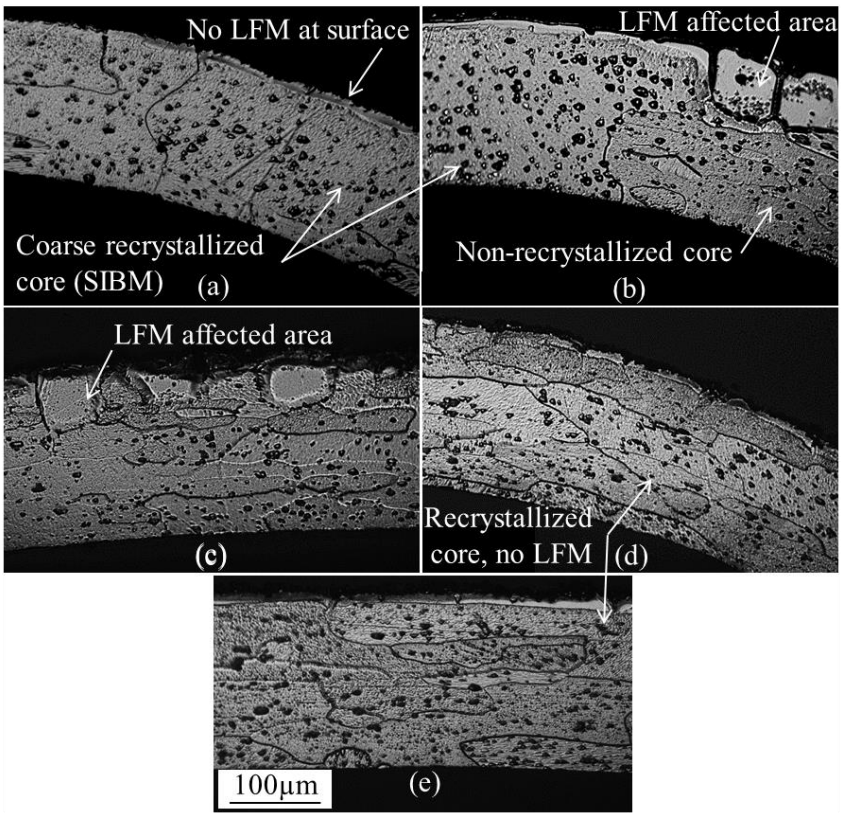

Figure 4. Post-braze microstructures from location 1 for (a) O-RT, (b) O-150°C, (c) O-250°C, (d) H24-RT, and (e) H24-250°C forming conditions

At location 2 in the channel inlet, the plastic strain reaches a relatively low level between 3.1% (H24-RT) and 4.1% (O-RT). LFM and a non-recrystallized core were observed in the plates formed from O temper sheet at RT and 150°C (Figure 5a and b). A non-recrystallized core was also found at location 2 in the O temper plate formed at 250°C (not shown), although LFM was not observed. Similar to location 1, the H24 post-braze microstructure was insensitive to an increase in forming temperature, and a recrystallized core alloy with no LFM was observed at the surface (Figure 5c and d).

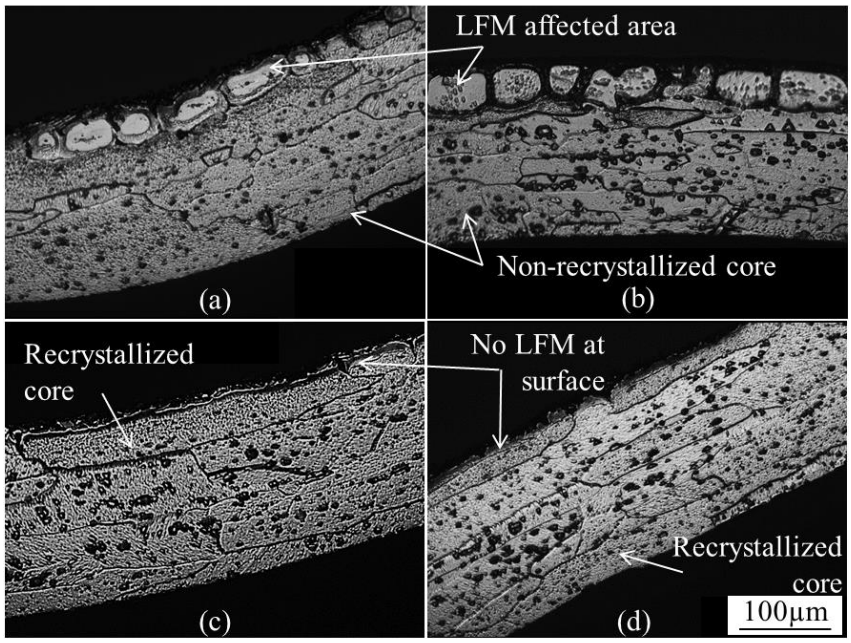

Figure 5. Post-braze microstructures from location 2 of the channel inlet for (a) O-RT, (b) O-150°C, (c) H24-RT, and (d) H24-250°C forming conditions

The post-braze microstructures at the faying surface of the formed dimples, where the local strain was estimated to be around 4% for all forming conditions (Figure 3d), are shown in Figure 6 for all forming conditions. A non-recrystallized core alloy and LFM attack were observed in the dimples of the O temper plates for all forming temperatures (Figure 6a-c), while the H24 sheet again had a recrystallized core alloy without an increased susceptibility to LFM (Figure 6d and e).

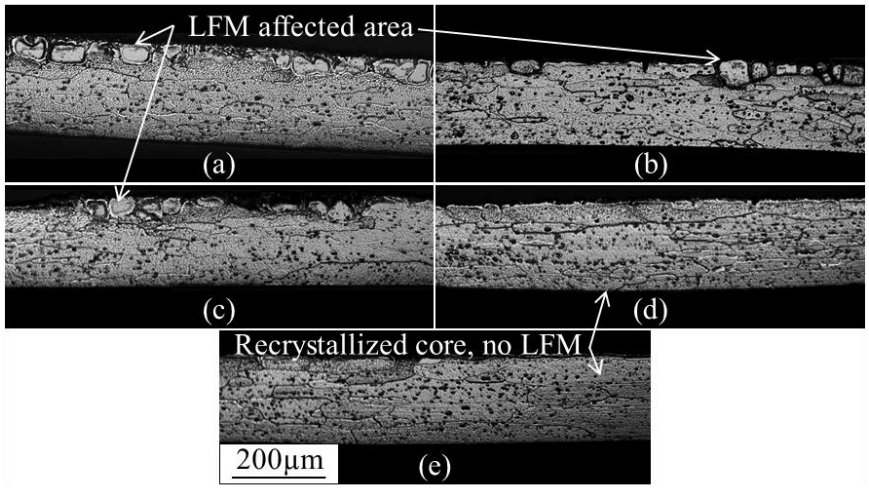

Figure 6. Post-brazed microstructures at the upper most surface of the dimples for the (a) O-RT, (b) O-150°C, (c) O-250°C, (d) H24-RT, and (e) H24-250°C forming conditions

Overall, the results from the formed battery plates align with the results from the warm deformed uniaxial coupons (Benoit et al., 2017, 2018), despite an orders of magnitude increase in the strain rate for the formed plates. The strain rate at the three locations of interest in the plate during deformation was

estimated from the FE model to be between 1.0×10^{-2} s^{-1} and 1.0×10^{-1} s^{-1}, while the strain rate in the prior tensile tests was on the order of 1.0×10^{-3} s^{-1}. For the plate formed from O temper sheet at RT, a non-recrystallized core and LFM were observed at locations with low strain ($\leq$ 4%) while negligible LFM and a core alloy recrystallized through SIBM were found in locations with higher levels of strain. For the O temper sheets formed at 150°C, LFM and a non-recrystallized core were observed, but over a slightly greater range of strains than for RT forming. At the highest levels of strain, the coarsened core alloy grains were observed in the plate (Figure 4b). Finally, in the O temper plates formed at 250°C, LFM was observed at locations with 4% strain and locations strained up to 10%. The driving force for the LFM phenomenon was proposed to be the reduction of stored deformation energy within the core alloy by the migrating liquid film (Woods, 1997; Wittebrood, 2009). Post-braze transmission electron microscopy images have shown that, in cases where LFM occurs, the core alloy undergoes recovery during brazing, rather than recrystallization, leaving sub-grains in the core, which are a source of excess stored energy. The extension of the regime over which LFM occurs when the sheets are warm formed has been attributed to the reduction in work hardening, and hence stored energy, during forming at elevated temperatures, making it increasingly difficult to reach the critical level of stored energy to trigger recrystallization during the brazing cycle. While warm forming can increase the material forming limits for the O temper sheet, it also extends the range of strains over which LFM will occur, and can shift its presence to critical brazing locations (Figure 4c). The resultant post-braze microstructure will vary with strain throughout a component made from O temper sheet, and will change with an increase in forming temperature; thus, warm forming will require careful consideration of the physical design of the components with respect to local strains imparted to the sheet, compared to RT formed components.

In contrast, the H24 sheet microstructure was characterized by a recrystallized core alloy and the absence of LFM, irrespective of location in the sheet. During processing of the H24 sheet, the sheet was rolled from an intermediate thickness to the final sheet thickness, with only partial annealing afterward, leaving the final sheet in a partially work hardened condition. Prior results have shown that the H24 core alloy, even in the as-received condition, has a greater level of stored energy compared to O temper sheet strained to 12% at RT (Benoit et al., 2017). Thus, the battery plates formed from the H24 sheet have a sufficiently high level of stored energy at all locations to trigger recrystallization during the brazing cycle, eliminating the driving force for LFM. Warm forming of the H24 sheet at 250°C did not alter the post-braze microstructure. During warm forming, the sheet was heated to 250°C and held for less than 1 minute; the temperature and time during warm forming were not high or long enough to cause significant recovery in the sheet. The warm formed sheet would, thus, still retain sufficient stored energy to induce recrystallization during brazing, and prevent the onset of LFM.

CONCLUSIONS

Warm forming has been shown to improve formability and reduce springback of multi-layered Al alloy sheets used in automotive heat exchanger production. However, the effect of increased forming temperature on brazing was not considered. In the current study, the brazing performance of simulated electric vehicle battery cooling plates formed from O and H24 sheet tempers was assessed on the basis of metallurgical reactions occurring within the sheet during brazing. The results of the study lead to the following conclusions:

1. The same metallurgical reactions observed in prior studies of uniaxial tensile specimens after simulated brazing were observed in the formed battery plates, despite much greater strain rates in the plates. Of particular importance is the balance between core alloy recrystallization and the occurrence of liquid film migration (LFM).

2. The post-braze microstructure in plates formed from O temper sheet varied with local strain in the plate, where the local stored energy determines if recrystallization or LFM occurs. Conversely, in plates formed from H24 sheet, the post-braze microstructure recrystallized at all locations and thus prevented LFM.

3. Warm forming will alter the post-braze microstructure of O temper sheets, by extending the range of strains over which LFM can occur, leading LFM to occur in critical locations in the plate such as the mating surfaces of the channel inlet.

4. Warm forming appears to be a viable manufacturing technique to reduce springback after forming of work hardened sheets, enabling improvements in component flatness without altering the post-braze microstructure. The duration and temperature during warm forming are not high enough to significantly reduce the stored deformation energy within the H24 sheet, allowing the warm formed sheet to recrystallize during the brazing cycle.

ACKNOWLEDGMENTS

Financial support from Automotive Partnership Canada (APC), the Natural Sciences and Engineering Research Council of Canada (NSERC), the Canada Foundation for Innovation, the Ontario Research Fund, and the Canada Research Chairs Secretariat is gratefully acknowledged. The authors would also like to express their gratitude to Chris Shore and Zeljko Gabriscek, both of Dana Canada Corporation, for their assistance in brazing the samples used in this study, as well as Dr. Carolyn Hansson of the University of Waterloo for providing editorial feedback in the preparation of this article.

REFERENCES

Bagheriasl, R., & Worswick, M. J. (2015). Formability of AA3003 brazing sheet at elevated temperatures: limiting dome height experiments and determination of forming limit diagrams. *International Journal of Material Forming, 8*(2), 229-244.

Bagheriasl, R., Ghavam, K., & Worswick, M. J. (2014). Formability improvement with independent die and punch temperature control. *International Journal of Material Forming, 7*(2), 139-154.

Bellier, S. P., & Doherty, R. D. (1977). The structure of deformed aluminium and its recrystallization-investigations with transmission kossel diffraction. *Acta Metallurgica , 25*(5), 521-538.

Benoit, M. J., Kaur, R., Wells, M. A., Jin, H., Shalchi Amirkhiz, B., & Winkler, S. (2018). Sagging resistance of warm formed aluminum brazing sheet. *Journal of Materials Processing Technology, 254*(4), 353-360.

Benoit, M. J., Whitney, M. A., Wells, M. A., Jin, H., & Winkler, S. (2017). Liquid film migration in warm formed aluminum brazing sheet. *Metallurgical and Materials Transactions A, 48*(10), 4645-4654.

Cheadle, B. E., & Dockus, K. F. (1988). *Inert atmosphere fluxless brazing of aluminum heat exchangers.* SAE Technical Paper 880446.

Corbin, S. F., Winkler, S., Turriff, D. R., & Kozdras, M. (2014). Analysis of fluxless, reactive brazing of Al alloys using differential scanning calorimetry. *Metallurgical and Materials Transactions A, 45*(9), 3907-3915.

Han, K. B. (2017). *A component-level study on effect of warm forming on formability and springback of aluminum alloy brazing sheet.* Waterloo: University of Waterloo.

Han, K. B., George, R., Kurukuri, S., Worswick, M. J., & Winkler, S. (2017). Springback of aluminum alloy brazing sheet in warm forming. *ESAFORM* . Dublin.

Livermore Software Technology Corporation. (2015). *LS-DYNA keyword user's manual volume I.* Livermore: LSTC.

Verma, R., George, R., Kurukuri, S., Worswick, M., & Winkler, S. (2015). Warm forming process study for reducing springback in aluminum alloy brazing sheets. *International Deep Drawing Research Group (IDDRG).* Shanghai.

Wittebrood, A. (2009). *Microstructural changes in brazing sheet due to solid-liquid interaction.* Delft: Delft University of Technology.

Wittebrood, A., Desikan, S., Boom, R., & Katgerman, L. (2006). Liquid film migration in aluminium brazing sheet? *International Conference on Aluminum Alloys (ICAA) 10. 519-521*, pp. 1151-1156. Vancouver: Materials Science Forum.

Woods, R. (1997). Liquid film migration during aluminum brazing. *Vehicle Thermal Management Systems (VTMS) 3.* Indianapolis.

Yang, H. S., & Woods, R. (1997). Mechanisms of liquid film migration (LFM) in aluminum brazing sheet. *Vehicle Thermal Management Systems (VTMS) 3.* Indianapolis.

Zhao, H., & Woods, R. (2013). Controlled atmosphere brazing of aluminum. In D. Sekulic, *Advances in Brazing: Science, Technology and Applications* (pp. 280-318). Oxford: Woodhead Publishing .